# A New Tropospheric Propagation Delay Mapping Function for Elevation Angles Down to 2°

Jiming Guo, *School of Geodesy and Geomatics, Wuhan University, China*
Richard B. Langley, *Department of Geodesy and Geomatics Engineering, University of New Brunswick, Canada*

## BIOGRAPHY

Jiming Guo was a visiting scholar in the Department of Geodesy and Geomatics Engineering at the University of New Brunswick (UNB) from June 2002 to June 2003. He has B.Sc. and M.Sc. degrees in Surveying Engineering from Wuhan Technical University of Surveying and Mapping and a Ph.D. in Satellite Geodesy from Wuhan University. He has been lecturing, researching and developing software in geodesy and geomatics at Wuhan since 1990.

Richard Langley is a professor in the Department of Geodesy and Geomatics Engineering at UNB, where he has been teaching since 1981. He has a B.Sc. in applied physics from the University of Waterloo and a Ph.D. in experimental space science from York University, Toronto. Prof. Langley has been active in the development of GPS error models since the early 1980s and is a contributing editor and columnist for GPS World magazine.

## ABSTRACT

The performance of tropospheric propagation delay prediction models used for microwave radiometric systems such as GPS typically degrades at very low elevation angles. In part, this is due to design considerations. The mapping functions used in the models to map the zenith delay prediction to the signal slant path were designed to be used above a limiting elevation angle. In the case of the Black and Eisner (B&E) mapping function, for example, its authors recommended its use for elevation angles of 7° and above. The B&E mapping function is used in computing the tropospheric delay in receivers which obtain error corrections from the Wide-area Augmentation System (WAAS) and other compatible space-based augmentation systems. This function was selected in the interest of computation simplicity and the need to provide delay corrections only for elevation angles above 5°. Through comparisons with ray tracing of global radiosonde profiles, the mean accuracy of the B&E mapping function (multiplied by zenith delay) has been assessed to be about 12 cm at an elevation angle of 6° and about 240 cm at 2°. On the other hand, the more modern, albeit more complex, Niell mapping function, which was originally proposed for the WAAS algorithm, has only a centimetre-level mean error at an elevation angle of 2°.

In this paper, we report on an investigation to determine the error of several mapping functions, including the B&E function, at elevation angles as low as 2° and present a new model, UNBabc, which has better low-elevation-angle performance than B&E and requires only slightly more computation time.

## INTRODUCTION

The mapping function of the neutral atmosphere propagation delay is used to map the zenith delay to the elevation-angle-dependent slant delay [Langley, 2002]. The existing mapping functions can be classified into two groups according to the application. One is the geodetic-survey oriented group; the other is the navigation-oriented group. Functions in the first group are more accurate but generally more complex and they find their major use in static data post-processing. The mapping functions developed by Davis et al. [1985], Ifadis [1986], Herring [1992] (hereafter called MTT), and Niell [1996] (hereafter called NMF) are examples of this group. Most of the mapping functions in this group, except NMF, need surface meteorological data – either observed or standard default values. The functions in the second group are simpler but usually less accurate. They are typically used for real-time navigation data processing. The Chao [1972], Black and Eisner [1984] (hereafter called B&E), and Foelsche and Kirchengast [2002] (hereafter called F&K) mapping functions are examples from the second group. Meteorological data is not needed for the second group of functions. The original atmospheric delay model

UNB3 [Collins, 1999] adopted the NMF algorithms for its mapping functions. The UNB3 model was adopted for use in satellite-based-augmentation-system (SBAS)-capable GPS receivers but the NMF mapping functions were replaced by the B&E function for the sake of simplicity and reduced computational burden [RTCA SC-159, 1999]. In this paper, we present the results of an investigation of the performance of the B&E function and propose a new function (UNBabc) which is more accurate than B&E and is only slightly more complex and therefore suitable for use in receiver firmware for modeling the effect of neutral atmosphere propagation delay.

Most of the geodetic-quality mapping functions use the continued fraction form. This functional form for the mapping function was first proposed by Marini [1972] and later on further developed by Chao [1972], Davis et al. [1985], Ifadis [1986], Herring [1992] and Niell [1996]. The general form can be written as:

$$m_i(\varepsilon) = \cfrac{1}{\sin\varepsilon + \cfrac{a_i}{\sin\varepsilon\,(or\ \tan\varepsilon) + \cfrac{b_i}{\sin\varepsilon + \cfrac{c_i}{\sin\varepsilon + \ldots}}}} \qquad [1]$$

where ε is the elevation angle and $a_i$, $b_i$, $c_i$, etc. are the mapping function parameters and may be constants or functions of other variables. Alternatively, the mapping function can be normalized to yield a value of unity at the zenith:

$$m_i(\varepsilon) = \cfrac{1 + \cfrac{a_i}{1 + \cfrac{b_i}{1 + \cfrac{c_i}{1 + \ldots}}}}{\sin\varepsilon + \cfrac{a_i}{\sin\varepsilon + \cfrac{b_i}{\sin\varepsilon + \cfrac{c_i}{\sin\varepsilon + \ldots}}}} \qquad [2]$$

All the parameters in the mapping function can be estimated by least-squares fitting with ray-tracing delay values (including hydrostatic and non-hydrostatic components and incorporating the effects of ray bending) at various elevation angles. Typically, one set of parameters is used to establish a hydrostatic mapping function (for i=h, the ray bending is usually included in this part), and another set of parameters is used for the non-hydrostatic mapping function (for i=nh).

The Chao model is a 2-term truncated form of the continued fraction and the second sine function is replaced by the tangent function so that the mapping function scale factor is 1 at the zenith. The other four models mentioned are 3-term truncated continued fractions.

The B&E and F&K mapping functions are analytic models. The B&E mapping function, currently adopted by the Wide-Area Augmentation System and other SBAS providers, is given by:

$$m(\varepsilon) = \frac{1.001}{\sqrt{0.002001 + \sin^2\varepsilon}} \qquad [3]$$

It is based on the quartic profile developed by Black and Eisner [1984]. The F&K mapping function is based on geometric relationships of the straight-line ray path length and the atmosphere effective height [Foelsche and Kirchengast, 2002]. It has a form given by:

$$m(\varepsilon) = (\frac{R_e}{H_{atm}} + 1)[\cos(\arcsin(\tilde{r}\cos\varepsilon) - \tilde{r}\sin\varepsilon]$$
$$\tilde{r} = \frac{R_e}{R_e + H_{atm}}$$
$$R_e = 6371km,\ H_{atm} = 14.5km \qquad [4]$$

The parameters and the effective elevation angle range for the models are summarized in Table 1.

The Ifadis, MTT and NMF functions constitute the "best" class [Mendes, 1999], but the first two need meteorological data for best performance. So we don't consider the Ifadis and MTT functions for the rest of our analysis. The NMF, Chao, B&E and F&K functions can be applied for navigation purpose without the need of actual meteorological data. However, NMF is perhaps a little too complex for some applications while the Chao, B&E, F&K functions are biased at very low elevation angles. The objective of our work was to find a model which would have good performance for elevation angles down to $2^o$ and also be simple enough for real-time implementation in the computation-limited receiver.

## NEW MAPPING FUNCTIONS

Considering the generally good performance of the mapping functions based on the continued fraction form, we adopted equation (2) as our base model and focused on the form of the three parameters a, b, and c. In order to estimate them, we ray-traced the refractivity profiles computed from the pressure, temperature and relative humidity profiles from balloon flights launched from 51 radiosonde stations in North America over a period of 5 years (1992-1996: 51 stations for 1992-1994, data from only 49 of the 51 stations were available for 1995, and data from only 42 of the 51 stations are available for 1996). Most of the stations launched radiosondes twice daily, every day of the year.

There are total of 160,243 radiosonde profiles for the selected data set. For each profile, the ray tracing was done at elevation angles of 1, 2, 3, 4, 5, 6, 7, 8, 9, 10, 20, 30, 40, 50, 60, 70, 80, and 90° to generate both hydrostatic and non-hydrostatic slant delays. The geographical distribution of the 51 stations is shown in Figure 1. The orthometric heights of the stations range from 2 m to 2234 m.

Due to the height limitation of ~30 km for the radiosonde balloons, the profiles ended well below the top of the neutral atmosphere. The upper part of the atmosphere from the last radiosonde reported level to ~80 km is approximated by the CIRA86 atmospheric model [Fleming et al., 1988].

From the ray tracing delay values, we produced two models. The first (UNBabc) has a 3-term continued fraction form. From a series of analyses, we concluded that parameter $a$ is sensitive to the orthometric height ($H$) and latitude ($\phi$) of the station whereas parameters $b$ and $c$ could be represented by constants. The least-squares estimated parameters for the hydrostatic function are

$a_h$= (1.18972-0.026855 H+ 0.10664 cos ϕ)/1000
$b_h$= 0.0035716
$c_h$= 0.082456

and

$a_{nh}$= (0.61120-0.035348 H-0.01526 cos ϕ)/1000
$b_{nh}$= 0.0018576
$c_{nh}$= 0.062741
for the non-hydrostatic component.

Another model we investigated has a 2-term continued fraction form. This model, called UNBab, considers both $a$ and $b$ as functions of $H$ and $\phi$ and is expressed as:

$a_h$= (1.53804-0.039491 H + 0.17020 cos ϕ)/1000
$b_h$= (50.0724-0.814759 H + 2.35232 cos ϕ)/1000
for the hydrostatic component, and

$a_{nh}$= (0.73537-0. 041172 H -0.00202 cos ϕ)/1000
$b_{nh}$= (32.5627-0. 670636H -0.15502 cos ϕ)/1000
for the non-hydrostatic component.

The functional forms of UNBabc and UNBab are summarized in Table 1. Slant delays were computed using the ray-traced vertical delays together with the derived mapping functions and compared to the ray-traced slant delays for elevation angles of 2 through 10° and for 20°. The results are shown in Table 2. The mean biases and r.m.s. errors of UNBabc are consistently smaller than those of UNBab for all elevation angles.

Table 1. The parameters and the effective elevation angle range for various mapping functions

| **Model** | **a** | **b** | **c** | **ε** | **$\varepsilon_{min}$ (°)** |
|---|---|---|---|---|---|
| Chao | constant | constant | no | yes | 10 |
| Ifadis | $F_{ia}$ (P,t,e) | $F_{ib}$ (P,t,e) | constant | yes | 2 |
| Davis | $F_{da}$ (P,t,e,$H_t$,α) | $F_{db}$ (P,t,e,$H_t$,α) | constant | yes | 5 |
| MTT | $F_{ma}$ (φ,H,t) | $F_{mb}$ (φ,H,t) | $F_{hc}$ (φ,H,t) | yes | 3 |
| NMF | $F_{na}$ (φ,H,doy) | $F_{nb}$ (φ,H,doy) | $F_{nc}$ (φ,H,doy) | yes | 3 |
| B&E | no | no | no | yes | 7 |
| F&K | no | no | no | yes | 6 |
| UNBabc | $F_{1a}$(ϕ,H) | constant | constant | yes | 2 |
| UNBab | $F_{2a}$(ϕ,H) | $F_{2b}$(ϕ,H) | no | yes | 2 |

P: surface total pressure, t: surface temperature, e: water vapor pressure, $H_t$: tropopause height, α: temperature lapse rate, φ: station latitude, H: station orthometric height, doy: day of year, F (·): function.

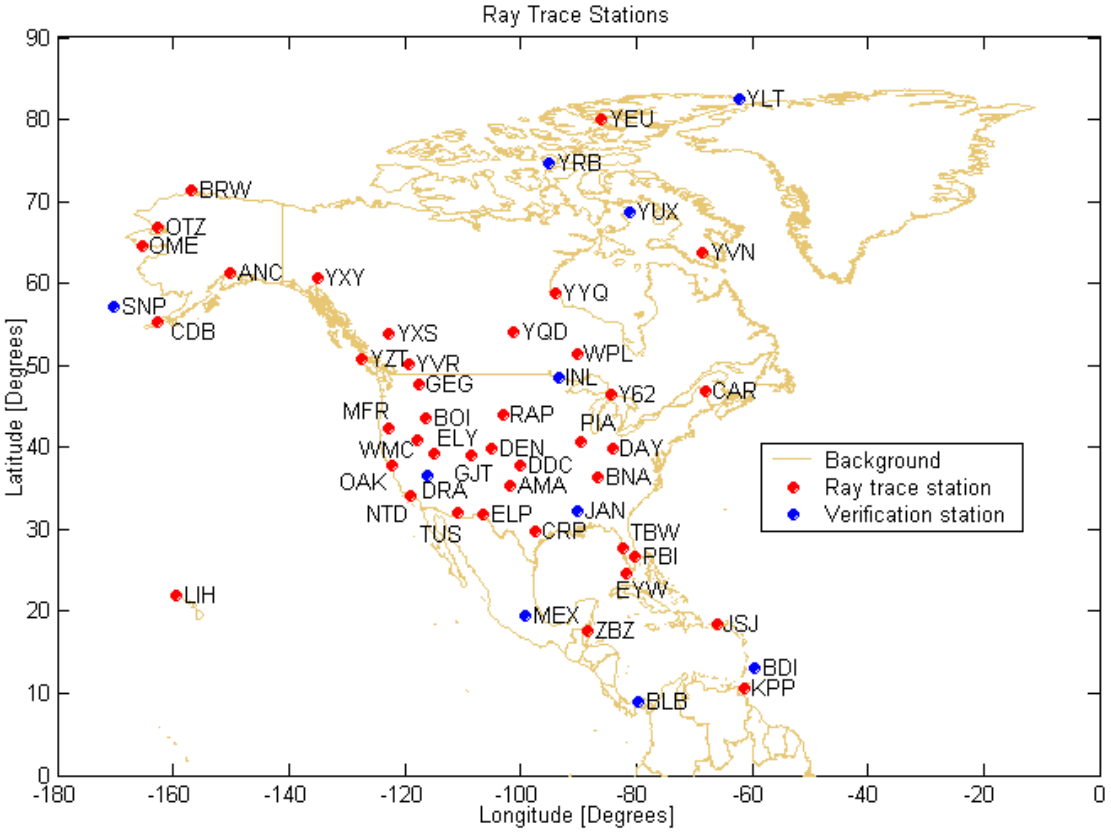


Fig.1 Distribution of radiosonde stations. Note that the verification stations were also used to determine the UNBabc and UNBab function parameters.

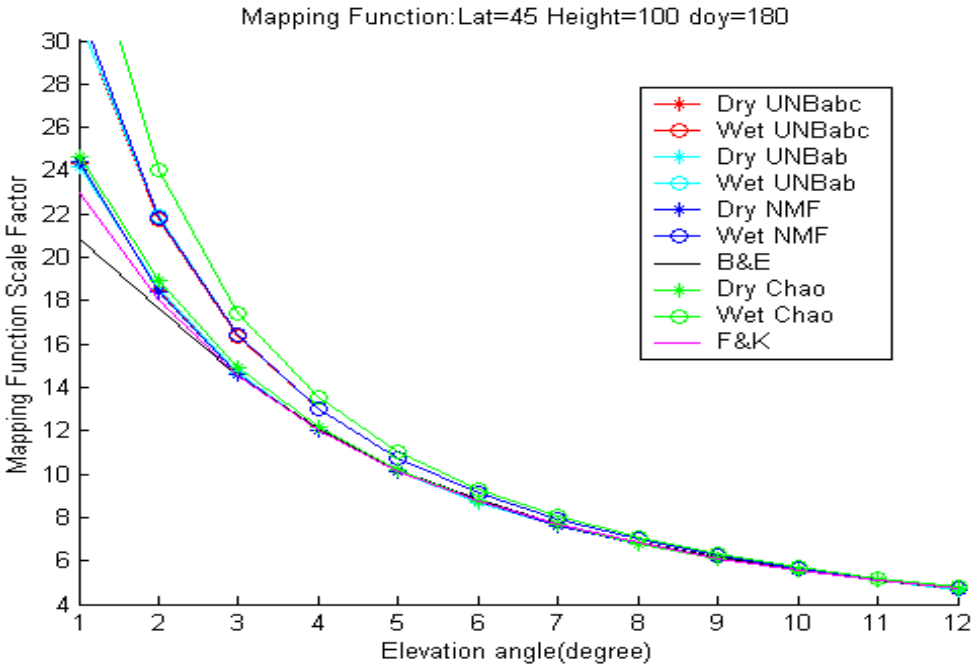


Fig. 2. Comparison of mapping function values for a specific latitude, height, and day of year (for those functions requiring this input).

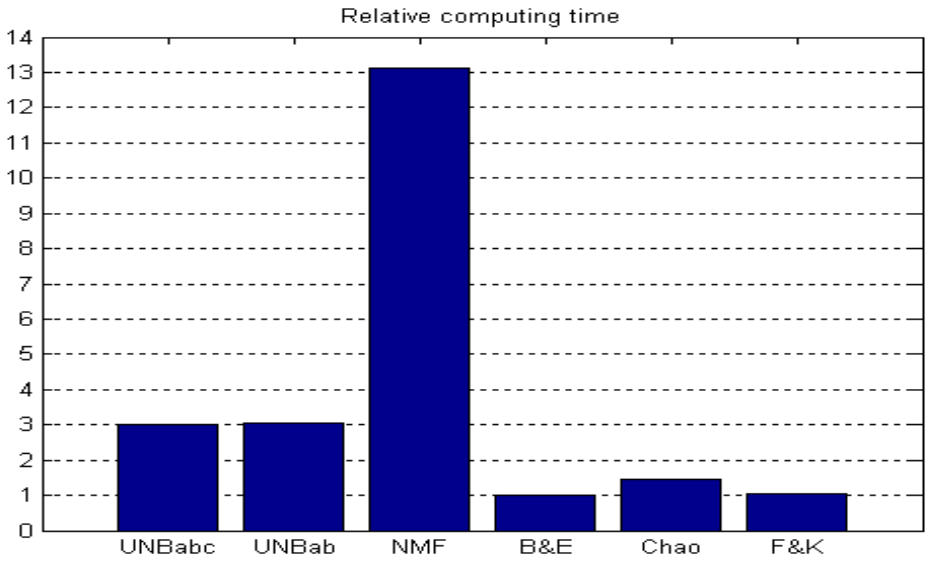


Fig. 3. The relative computing time of the new mapping functions compared to existing functions.

Table 2. The mean bias and r.m.s. of UNBabc and UNBab (cm)

| Elev. (°) | UNBabc | | UNBab | |
|---|---|---|---|---|
| | **Bias** | **r.m.s.** | **Bias** | **r.m.s.** |
| 2 | 3.82 | 22.17 | 20.62 | 29.20 |
| 3 | 2.15 | 11.85 | 7.67 | 13.66 |
| 4 | 1.07 | 6.86 | -1.35 | 6.91 |
| 5 | 0.38 | 4.23 | -5.18 | 6.60 |
| 6 | 0.02 | 2.77 | -6.25 | 6.68 |
| 7 | -0.14 | 1.90 | -6.13 | 6.24 |
| 8 | -0.20 | 1.37 | -5.56 | 5.54 |
| 9 | -0.21 | 1.01 | -4.86 | 4.81 |
| 10 | -0.19 | 0.77 | -4.18 | 4.12 |
| 20 | 0. 00 | 0.10 | -0.92 | 0.93 |

## VERIFICATION

To get a first impression of how the UNBabc and UNBab mapping functions compare with the other functions listed in Table 1, we have computed the function scale factors for elevation angles of 1 through 12° for representative conditions (for those functions using these parameters): latitude = 45°, height = 100m, and day of year = 180. The results are shown in Figure 2. In the figure, the NMF results almost exactly overlie the UNBabc and UNBab results.

In order to evaluate the performance of UNBabc and UNBab in both accuracy and computing time, we have compared them with the other functions listed in Table 1. The performances were determined by comparing the slant delays predicted by the mapping functions with those obtained by ray tracing through the data from a subset of the radiosonde stations for the year 1992. The stations used for the analysis were selected to give a good geographical representation as well as a range of station heights. The relative computing time for each function is shown in Figure 3. In the case of mapping functions with both hydrostatic and non-hydrostatic components, the computing time is for both components. The mean biases of the functions (multiplied by the ray-traced zenith delay for each profile) at elevation angles of 2, 4, 7, 10, 30, and 60° for each station are shown in Figure 4. The stations are listed according to increasing latitude from BLB (Bilbao, Panama) to YLT (Alert, Canada).

The overall mean biases and r.m.s. errors for each mapping function (multiplied by the ray-traced zenith delay for each profile) from the 10-station 1992 data set are shown in Figures 5 and 6 respectively. Again, for those functions which have separate hydrostatic and non-hydrostatic components, the values shown are for the total delay. It is interesting to note that the mean accuracy of B&E is about 12 cm at an elevation angle of 6° and about 240 cm at 2° whereas UNBabc and NMF have a sub-centimetre mean error at an elevation angle of 6° and centimetre-level mean error even at an elevation angle of 2°.

(a)

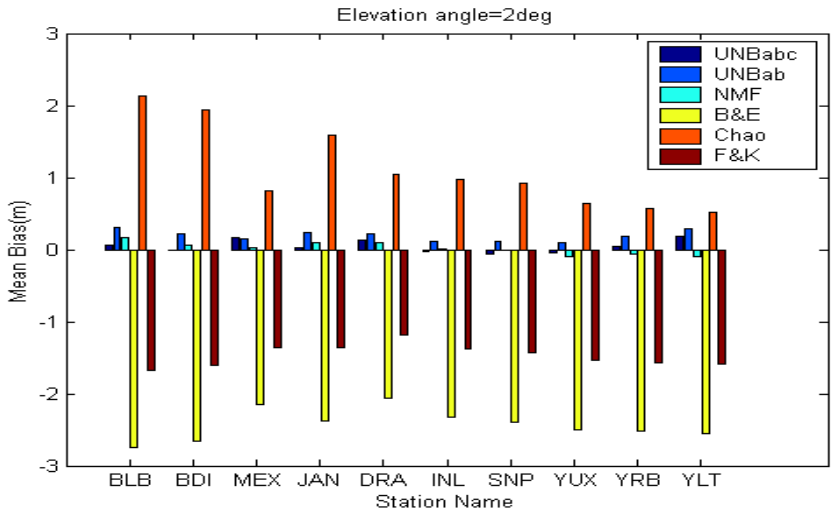
Elevation angle=2deg
Mean Bias(m)
Station Name
UNBabc
UNBab
NMF
B&E
Chao
F&K
BLB BDI MEX JAN DRA INL SNP YUX YRB YLT

(b)

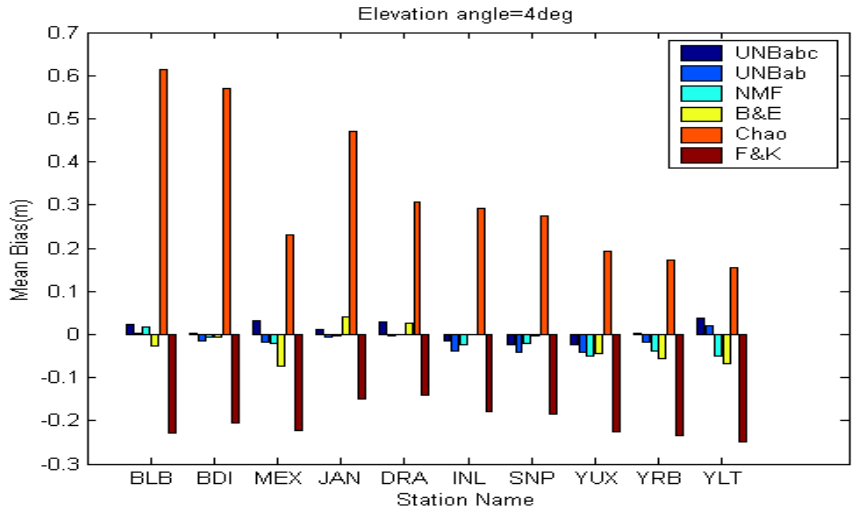
Elevation angle=4deg
Mean Bias(m)
Station Name
UNBabc
UNBab
NMF
B&E
Chao
F&K
BLB BDI MEX JAN DRA INL SNP YUX YRB YLT

(c)

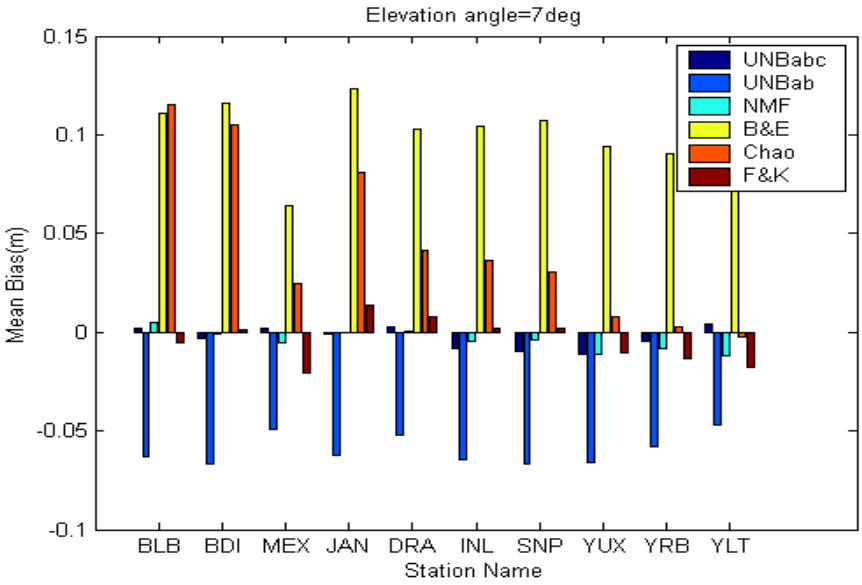
Elevation angle=7deg
Mean Bias(m)
Station Name
UNBabc
UNBab
NMF
B&E
Chao
F&K
BLB BDI MEX JAN DRA INL SNP YUX YRB YLT

(d)

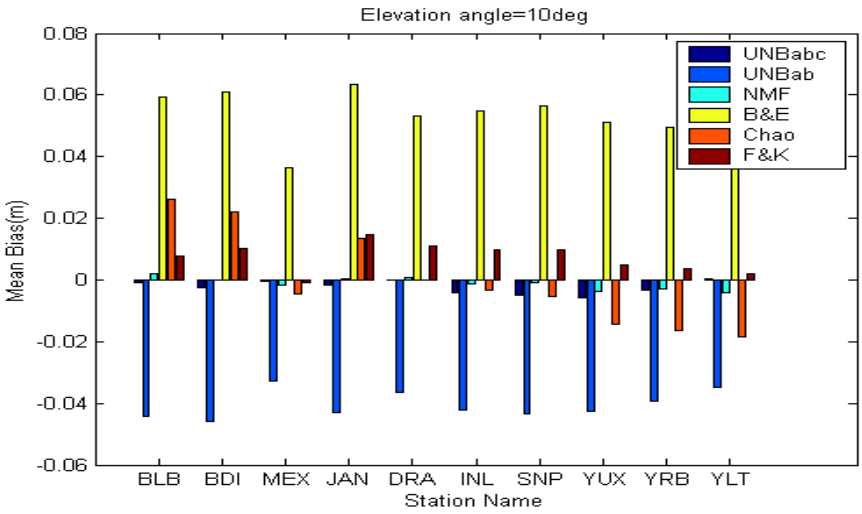


(e)

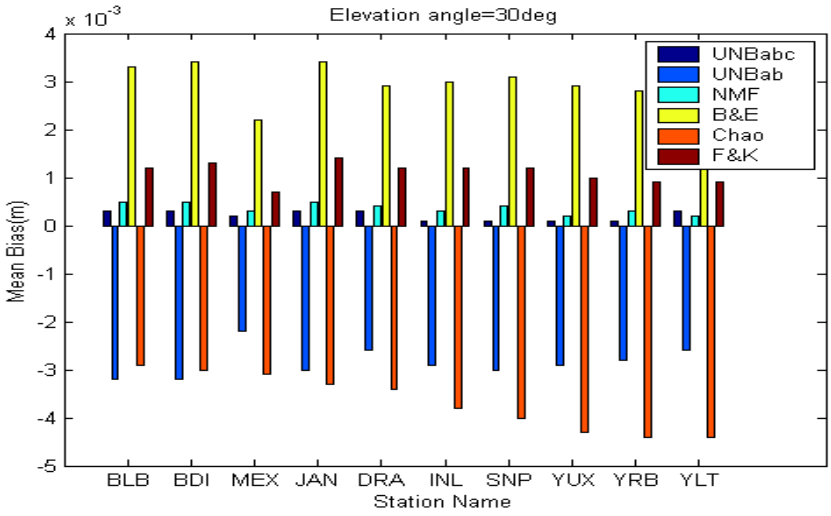


(f)

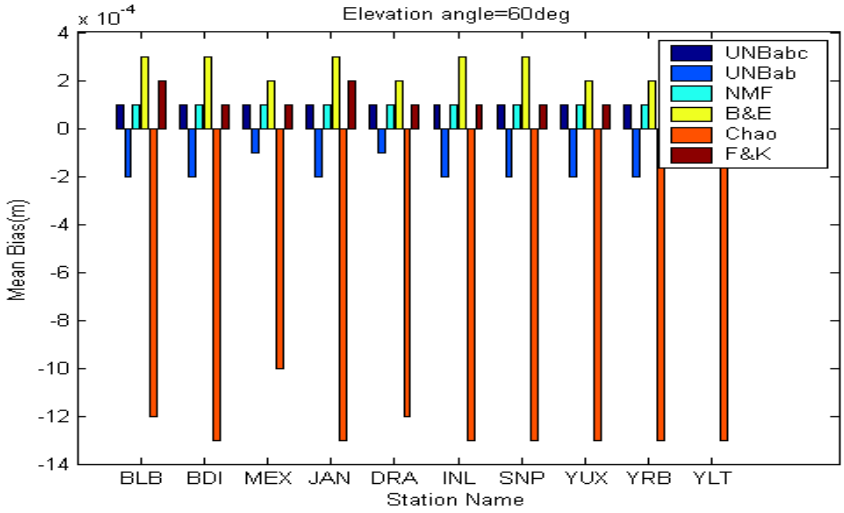


Fig. 4. Mean biases of mapping functions (multiplied by vertical delay) at 10 radiosonde stations for elevation angles of (a) 2°, (b) 4°, (c) 7°, (d) 10°, (e) 30°, and (f) 60°.

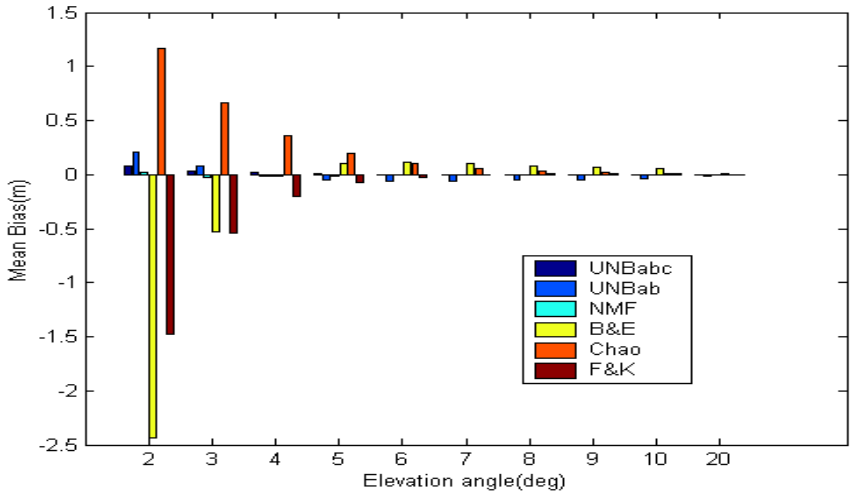


Fig. 5. Mean biases of mapping functions (multiplied by zenith delay) at 10 radiosonde sites during 1992.

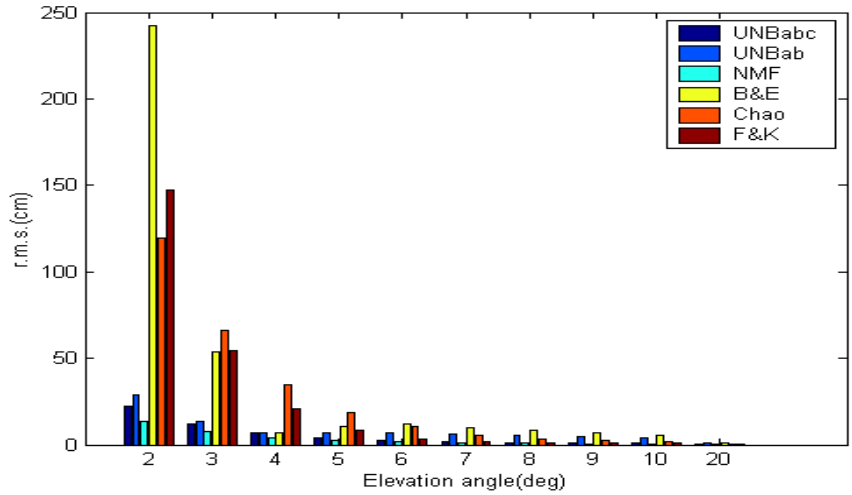


Fig. 6. r.m.s. errors of mapping functions (multiplied by zenith delay) at 10 radiosonde sites during 1992.

From Figures 2 to 6, we draw the following conclusions:

1) The rank by computing time is (fastest to slowest): B&E and F&K; Chao; UNBabc and UNBab; NMF. The ratios are approximately 1:1.5:3:13. Both UNBabc and UNBab take only about 3 times as long to compute values for both the hydrostatic and non-hydrostatic functions as the B&E function and are more than four times faster than NMF.

2) The rank by accuracy (bias – smallest to largest) is: NMF; UNBabc; UNBab, F&K, B&E, and Chao (the differences among these four are small). In this latter group of four mapping functions, the individual functions seem to have smallest biases at particular elevation angles: UNBab is best at 2-3°, B&E is good at 4°, while F&K is the best above 6°.

3) At very low elevation angles (2° and 3°), due to the neglect of ray bending and water vapor influence, the B&E and F&K functions have large biases. The curves of Chao, B&E, F&K diverge from those of NMF and UNBabc at the low elevation angles.

4) The Niell mapping function is the best in accuracy, but it takes 13 times longer to compute than B&E.

## CONCLUSION

From its overall performance, we conclude that UNBabc is the best candidate for a GNSS receiver built-in mapping function. It takes much less time to compute than NMF does and has much better accuracy than B&E. The performance of UNBab (and Chao) shows that the 2-term continued fraction form is not flexible enough for a mapping function to cover the whole elevation angle range down to 2°.

**ACKNOWLEDGMENTS**

The ray tracing software used in our work is a modified version of the software developed by J.L. Davis, T.A. Herring, and A.E. Niell. The modifications were performed by J.P. Collins and V.B. Mendes. We also used RAOBSCAN, a software module written by Collins. We thank Niell, Mendes, and Collins for providing the software and for their helpful advice. The support of NavCanada and Chinese Scholarship Committee is gratefully acknowledged.

**REFERENCES**

Black, H.D and A. Eisner (1984). "Correcting satellite Doppler data for tropospheric effects". *Journal of Geophysical Research*, Vol. 89, No. D2, pp. 2616-2626.

Chao, C.C. (1972). *A Model for Tropospheric Calibration from Daily Surface and Radiosonde Balloon Measurement*. Technical Memorandum 391-350, Jet Propulsion Laboratory, Pasadena, CA.

Collins, J.P. (1999). *Assessment and Development of a Tropospheric Delay Model for Aircraft Users of the Global Positioning System.* M.Sc.E. thesis, Department of Geodesy and Geomatics Engineering Technical Report No. 203, University of New Brunswick, Fredericton, N.B., Canada, 174 pp.

Davis, J.L., T.A. Herring, I.I. Shapiro, A.E.E. Rogers, and G. Elgered (1985). "Geodesy by radio interferometry: Effects of atmospheric modeling errors on estimates of baseline length". *Radio Science*, Vol. 20, pp. 1593-1607.

Fleming, E.L., S. Chandra, M.R. Schoeberl and J.J. Barnet (1988). *Monthly Mean Global Climatology of Temperature, Wind, Geopotential Height and Pressure for 0-120km*. NASA TM-100697, Goddard Space Flight Centre, Greenbelt, MD.

Foelsche, U. and G. Kirchengast (2002). "A simple 'geometric' mapping function for the hydrostatic delay at radio frequencies and assessment of its performance". *Geophysical Research Letters*, Vol.29, No.10, pp. 1111-1114.

Herring, T.A. (1992). "Modeling atmospheric delays in the analysis of space geodetic data". *Proceedings of the Symposium on Refraction of Transatmospheric Signals in Geodesy*, Eds. J.C. De Munck and T.A.Th. Spoelstra, Netherlands Geodetic Commission, Publications on Geodesy, No. 36, pp.157-164.

Ifadis, I.M. (1986). The Atmospheric Delay of Radio Waves: Modeling the Elevation Dependence on a Global Scale. *Technical Report 38L*, Chalmers University of Technology, Gothenborg, Sweden.

Langley, R.B. (2002). *Monitoring the Ionosphere and Neutral Atmosphere with GPS*. Viewgraphs of invited presentation to the Canadian Association of Physicists Division of Atmospheric and Space Physics Workshop, Fredericton, N.B., 21-23 February 2002.

Marini, J.W. (1972). "Correction of satellite tracking data for an arbitrary tropospheric profile". *Radio Science*, Vol. 7, No. 2, pp. 223-231.

Mendes, V.B. (1999). *Modeling the Neutral-atmosphere Propagation Delay in Radiometric Space Techniques*. Ph.D. dissertation, Department of Geodesy and Geomatics Engineering Technical Report No. 199, University of New Brunswick, Fredericton, N.B., Canada.

Niell, A.E. (1996). "Global mapping functions for the atmosphere delay at radio wavelengths". *Journal of Geophysical Research*, Vol. 101, No. B2, pp. 3227-3246.

RTCA SC-159, (1999). *Minimum Operational Performance Standards for Global Positioning System/Wide Area Augmentation System Airborne Equipmen*t, RTCA/DO-229B, RTCA Inc., Washington, D.C.